

Reanalysis of energy band structure in the type-II quantum wells

Xinxin Li(李欣欣), Zhen Deng(邓震), Yang Jiang(江洋), Chunhua Du(杜春花), Haiqiang Jia(贾海强), Wenxin Wang(王文新), and Hong Chen(陈弘)

Citation: Chin. Phys. B, 2024, 33 (**6**): 067302. DOI: 10.1088/1674-1056/ad36bc
Journal homepage: http://cpb.iphy.ac.cn; http://iopscience.iop.org/cpb

What follows is a list of articles you may be interested in

Light-modulated graphene-based φ_0 Josephson junction and -φ_0 to φ_0 transition

Renxiang Cheng(程任翔), Miao Yu(于苗), Hong Wang(汪洪), Deliang Cao(曹德亮), Xingao Li(李兴鳌), Fenghua Qi(戚凤华), and Xingfei Zhou(周兴飞)

Chin. Phys. B, 2024, 33 (**2**): 027302. DOI: 10.1088/1674-1056/ad04c5

Electric modulation of the Fermi arc spin transport via three-terminal configuration in topological semimetal nanowires

Guang-Yu Zhu(祝光宇), Ji-Ai Ning(宁纪爱), Jian-Kun Wang(王建坤), Xin-Jie Liu(刘心洁), Jia-Jie Yang(杨佳洁), Ben-Chuan Lin(林本川), and Shuo Wang(王硕)

Chin. Phys. B, 2024, 33 (**1**): 017305. DOI: 10.1088/1674-1056/ace157

Enhanced thermoelectric properties in two-dimensional monolayer Si_2BN by adsorbing halogen atoms

Cheng-Wei Wu(吴成伟), Changqing Xiang(向长青), Hengyu Yang(杨恒玉), Wu-Xing Zhou(周五星), Guofeng Xie(谢国锋), Baoli Ou(欧宝立), and Dan Wu(伍丹)

Chin. Phys. B, 2021, 30 (**3**): 037304. DOI: 10.1088/1674-1056/abd163

Electronic properties of silicene in BN/silicene van der Waals heterostructures

Ze-Bin Wu(吴泽宾), Yu-Yang Zhang(张余洋), Geng Li(李更), Shixuan Du(杜世萱), Hong-Jun Gao(高鸿钧)

Chin. Phys. B, 2018, 27 (**7**): 077302. DOI: 10.1088/1674-1056/27/7/077302

Gap opening and tuning in single-layer graphene with combined electric and magnetic field modulation

Lin Xin(林鑫), Wang Hai-Long(王海龙), Pan Hui(潘晖), and Xu Huai-Zhe(许怀哲)

Chin. Phys. B, 2011, 20 (**4**): 047302. DOI: 10.1088/1674-1056/20/4/047302

RAPID COMMUNICATION

Reanalysis of energy band structure in the type-II quantum wells

Xinxin Li(李欣欣)[1,2,†], Zhen Deng(邓震)[1,2,3,†], Yang Jiang(江洋)[1,2], Chunhua Du(杜春花)[1,2,3], Haiqiang Jia(贾海强)[1,2,4], Wenxin Wang(王文新)[1,2,4], and Hong Chen(陈弘)[1,2,3,4,‡]

[1] *Key Laboratory for Renewable Energy, Beijing Key Laboratory for New Energy Materials and Devices, Beijing National Laboratory for Condensed Matter Physics, Institute of Physics, Chinese Academy of Sciences, Beijing* 100190, *China*

[2] *Center of Materials and Optoelectronics Engineering, University of Chinese Academy of Sciences, Beijing* 100049, *China*

[3] *The Yangtze River Delta Physics Research Center, Liyang* 213000, *China*

[4] *Songshan Lake Materials Laboratory, Dongguan* 523808, *China*

(Received 18 March 2024; revised manuscript received 22 March 2024; accepted manuscript online 22 March 2024)

Band structure analysis holds significant importance for understanding the optoelectronic characteristics of semiconductor structures and exploring their potential applications in practice. For quantum well structures, the energy of carriers in the well splits into discrete energy levels due to the confinement of barriers in the growth direction. However, the discrete energy levels obtained at a fixed wave vector cannot accurately reflect the actual energy band structure. In this work, the band structure of the type-II quantum wells is reanalyzed. When the wave vectors of the entire Brillouin region (corresponding to the growth direction) are taken into account, the quantized energy levels of the carriers in the well are replaced by subbands with certain energy distributions. This new understanding of the energy bands of low-dimensional structures not only helps us to have a deeper cognition of the structure, but also may overturn many viewpoints in traditional band theories and serve as supplementary to the band theory of low-dimensional systems.

Keywords: energy band structure, type-II quantum wells, low-dimensional semiconductors

PACS: 73.20.At, 73.22.−f, 73.63.Hs **DOI:** 10.1088/1674-1056/ad36bc

1. Introduction

The band theory is one of the important theories in the semiconductor physics and device field,[1] and the band structure analyzing of the semiconductor holds significant importance for further understanding the optoelectronic characteristics and exploring its potential applications in optoelectronics.[2–4] In turn, it is also possible to manipulate the band structure to achieve the desired properties through doping,[5] composition change,[6,7] strain[8–10] and quantum confinement,[11,12] for special application requirements. Among the above methods, quantum confinement can only be achieved in low-dimensional systems, and various devices with adjusted wavelengths and high conversion efficiency have been developed with band engineering.[13–16] Unfortunately, the confinement behavior of carriers is harmful to develop high-performance optoelectronic devices based on interband transitions in classical theory, which believes that the photo-generated carriers in the low-dimensional materials cannot escape from the potential well to form the photocurrent due to the quantized energy levels.[17] Fortunately, in recent years, we have experimentally observed great carrier extraction efficiencies (more than 90%) in InGaN multi-quantum wells (MQWs),[18–20] InGaAs MQWs,[21,22] and other low-dimensional materials systems[23,24] in PIN structures. The relevant experimental data and simulation results indicate that the carriers in the well are not confined, but escape from the well.[25] Furthermore, most of the escaped carriers do not originate from the thermal excitation[26] or tunneling.[27] It is evident that the quantized energy levels of MQWs structure analyzed from the traditional band theory cannot explain this unconfined behavior, and thus the energy band of two-dimensional QWs urgently needs a reanalysis.

Generally, there are three different types of MQWs structures depending on the band alignment differences at interfaces between the barriers and wells. In the type-II band alignment, electrons and holes are confined in different layers.[28] In this work, we have reanalyzed the band structure of the type-II MQWs. Unlike discrete energy levels given in the classical band theory at a fixed wave vector, the reanalyzed energy band structure in this paper consists of subbands with certain energy distributions when the wave vectors of the entire Brillouin region (corresponding to the growth direction) are taken into account. As a new understanding of the energy band structure, it may overturn our previous recognition of quantum properties and serve as supplementary to the band theory of low-dimensional systems.

2. Results and discussion

The MQWs structure is a multilayer structure formed by alternating two nanofilms with different components. For the

[†]These authors contributed equally to this work.

[‡]Corresponding author. E-mail: hchen@iphy.ac.cn

© 2024 Chinese Physical Society and IOP Publishing Ltd

type-II MQWs structure, both the conduction-band edge and the valence-band edge of one material are lower than the corresponding band edges of the other material, resulting in electrons being confined to one material and holes being confined to the other, as shown in Fig. 1(a). Figure 1(a) is a schematic diagram of the energy bands of the type-II MQWs structure in real space. The discontinuity in the conduction-band edges of materials A and B confines electrons to material B, whereas the discontinuity in their valence-band edges confines holes to material A. According to the traditional band theory, the energy in the MQWs is split into discrete energy levels due to the quantum confinement effect. The red and green lines represent the quantized energy levels of electrons and holes, respectively, where the hole energy levels consist of light hole energy (light green line) and heavy hole energy (dark green line) due to the interaction of valence bands. It should be emphasized that during the process of obtaining the quantized energy levels based on the classical band theory in Fig. 1(a), a fixed $\boldsymbol{k}$ vector with extreme energy is selected as a representative to display the quantum behavior for simplification, while the other part in the dispersion is ignored. Although this simplified approach has been widely accepted and has confirmed its practicality in certain scenarios, the quantized energy levels obtained at a fixed wave vector cannot accurately reflect the actual energy band structure. The neglected parts should be reconsidered to have a more comprehensive representation of the band structure in type-II MQWs structure.

The energy dispersions of the materials A and B are given in Fig 1(b). Based on the phase equilibrium conditions, it is the chemical potential that determines the alignment of energy dispersions for an equilibrium heterojunction.[29] As we can see, both the electron energy and the hole energy dispersions of material A are lower than those of the adjoining material B, which is consistent with the definition of type-II MQWs structure. The difference in the electron dispersions or hole dispersions at the same $\boldsymbol{k}$ vector in Fig. 1(b) is called band offset,[28] which plays a crucial role in confining the motion of electrons or holes in the well, leading to the quantum behavior in Fig. 1(a). Considering all the band offsets at all $\boldsymbol{k}$ vectors, the real energy of carriers within the entire Brillouin zone should be the combination of the bulk energy dispersion and the additional quantized energy levels at all $\boldsymbol{k}$ vectors.

Distinct from the superlattice structure with strong coupling, the coupling between the wells can be ignored in the MQWs structure due to the thicker barrier layer.[30] Therefore, the analysis of the energy bands in the MQWs structure can usually be simplified into the analysis of a single QW structure. For the type-II MQWs structure in Fig. 1(a), the energy E_z along the growth direction (z direction) in the well consists of two parts as analyzed above:

$$E_z = E_z^{\mathrm{b}} + E_z^{\mathrm{s}}, \tag{1}$$

where E_z^{b} represents the energy resulting from the interaction of crystal cells in the bulk material, and E_z^{s} is quantum energy level caused by quantum confinement.

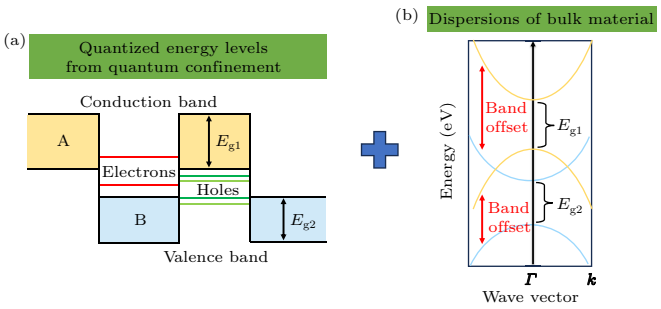


Fig. 1. (a) The quantized energy levels in real space caused by the quantum confinement in type-II MQWs structure. (b) The schematic diagram of the energy dispersions of materials A and B in (a) in $\boldsymbol{k}$-space.

The energy E_z^{b} is only related to the material itself, and can be calculated using the classical band theory with many methods, including the tight binding approximation method (TBA), the orthogonal plane-wave method (OPW), the $k \cdot p$ method, and the pseudopotential method.[31] The details of the calculation process are not shown here. As for the quantized energy E_z^{s} at all $\boldsymbol{k}$ vectors, the issue can be simplified to solve a one-dimensional potential well with finite depth. The Schrödinger equation for stationary states on the position basis in the well is given as[32]

$$\begin{aligned} &-\frac{\hbar^2}{2m^*_{(\boldsymbol{k}_z)}}\frac{\mathrm{d}^2}{\mathrm{d}z^2}\psi_{E_z^{\mathrm{s}}(\boldsymbol{k}_z)}(z) + V_{(\boldsymbol{k}_z)}(z)\,\psi_{E_z^{\mathrm{s}}(\boldsymbol{k}_z)}(z) \\ &= E^{\mathrm{s}}_{z\,(\boldsymbol{k}_z)}\psi_{E_z^{\mathrm{s}}(\boldsymbol{k}_z)}(z), \\ &V_{(\boldsymbol{k}_z)}(z) = \begin{cases} 0, & |z| < \dfrac{a}{2}, \\ V_{(\boldsymbol{k}_z)}, & \dfrac{l}{2} \geq |z| \geq \dfrac{a}{2}, \end{cases} \end{aligned} \tag{2}$$

where $m^*_{(\boldsymbol{k}_z)}$ is the effective mass of the carrier, z is the position in the well, $\boldsymbol{k}_z$ is the wave vector along the z direction, $\psi_{E_z^{\mathrm{s}}(\boldsymbol{k}_z)}(z)$ is the wave function of the particle corresponding to the quantization energy $E^{\mathrm{s}}_{z\,(\boldsymbol{k}_z)}$, $V_{(\boldsymbol{k}_z)}(z)$ is the well potential, and l is the period thickness of the quantum well, which is equal to the sum of the well thickness a and barrier thickness b.

It should be noted that the effective mass $m^*_{(\boldsymbol{k}_z)}$ and the well-potential $V_{(\boldsymbol{k}_z)}$ are both related to $\boldsymbol{k}_z$. The $m^*_{(\boldsymbol{k}_z)}$ can be obtained by taking two derivatives of the energy $E^{\mathrm{s}}_{z\,(\boldsymbol{k}_z)}$ with respect to $\boldsymbol{k}_z$ as[33]

$$m^*_{(\boldsymbol{k}_z)} = \frac{\hbar^2}{\left(\dfrac{\mathrm{d}^2 E_z^{\mathrm{b}}(\boldsymbol{k}_z)}{\mathrm{d}\boldsymbol{k}_z^2}\right)} \begin{cases} E_z^{\mathrm{b}} = E_z^{\mathrm{b-w}}, & |z| < \dfrac{a}{2}, \\ E_z^{\mathrm{b}} = E_z^{\mathrm{b-b}}, & \dfrac{l}{2} \geq |z| \geq \dfrac{a}{2}, \end{cases} \tag{3}$$

where $E_z^{\mathrm{b-w}}$ is the bulk energy dispersion of the well, and $E_z^{\mathrm{b-b}}$ is the bulk energy dispersion of the barrier.

The well potential $V_{(\boldsymbol{k}_z)}$ is determined by the band offset obtained from the difference of energy dispersions (as shown in Fig. 1(b)) according to the electron affinity rule:[34,35]

$$V_{(\boldsymbol{k}_z)} = E_z^{\mathrm{b-b}}{}_{(\boldsymbol{k}_z)} - E_z^{\mathrm{b-w}}{}_{(\boldsymbol{k}_z)}. \tag{4}$$

Therefore, the corresponding quantized energy levels E_z^{s} at different $\boldsymbol{k}$ vectors can be obtained by solving the above Schrödinger equation (2), which usually consists of writing the general forms of the wave functions inside and outside the well and then matching the values and slopes at the boundary to solve for the unknown constants.

To illustrate the proper band structure of type-II MQWs structure in a more intuitive way, a schematic diagram of the real energy dispersion of the structure is provided in Fig. 2(a), where the superposition process of the bulk energy dispersion and the quantized energy levels at all $\boldsymbol{k}_z$ vectors is clearly shown. In Fig. 2(a), the green line represents the energy dispersion of the bulk material along the z-direction (E_z^{b}), where the lowest energy is at $\boldsymbol{\Gamma}$ point. While the red line signifies the split energy levels at different vectors due to quantum confinement, for example, the ground state E_{z0}^{s}. The total energy at $\boldsymbol{k}_z$ will be the sum of the energy at $\boldsymbol{k}_z$ in the green line (from the bulk material) and the energy at $\boldsymbol{k}_z$ in the red line (from the confinement), corresponding to the energy of the red point on the blue line ($E_{z0}(\boldsymbol{k}_z)$). Obviously, this is consistent with quantization energy levels at a fixed $\boldsymbol{k}_z$ vector obtained from the classical band theory. However, when all $\boldsymbol{k}_z$ vectors in the Brillouin zone are taken into account, the real energy of carriers (E_{z0}) in the QW structure (blue line in Fig. 2(a)) exhibits a certain range of energy in the whole Brilluin zone. To further analyze the energy band of the type-II MQWs structure, the energy dispersion E_z in Fig. 2(a) is transformed into real space, as depicted in Fig. 2(b). Taking electrons in material B as an example, the red lines in the well in Fig. 2(b) are the quantized energy levels of electrons caused by the quantum confinement at $\boldsymbol{\Gamma}$ point. The energy dispersion E_{z0} in Fig. 2(a) becomes a band with a certain energy distribution in the real space, as shown by the blue shaded area in Fig. 2(b), with the red line located exactly at the bottom.

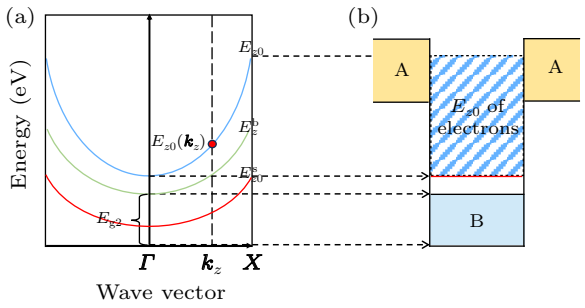


Fig. 2. (a) The schematic diagram of energy dispersion E_{z0} consists of the energy dispersion (E_z^{b}) of the bulk material and quantization energy E_z^{s} at all $\boldsymbol{k}_z$ vectors. (b) The energy band structure in the real space for electrons in the type-II MQWs structure from the energy dispersion E_{z0}.

Moreover, if the other quantized energy levels are considered within the whole Brillouin zone, for example, the $E_{z1}^{\mathrm{s}}(\boldsymbol{\Gamma})$ and $E_{z2}^{\mathrm{s}}(\boldsymbol{\Gamma})$, their dispersions will be distinguished due to the difference in the quantized energy levels, as shown in Fig. 3(a). The three blue curves with colors of light blue, medium blue, and deep blue represent the dispersions of the ground state (E_{z0}), the first state (E_{z1}), and the second state (E_{z2}), respectively. Their energies at $\boldsymbol{\Gamma}$ point, $E_{z0}(\boldsymbol{\Gamma})$, $E_{z1}(\boldsymbol{\Gamma})$, and $E_{z2}(\boldsymbol{\Gamma})$, agree well with the quantized energy levels given in the classical band theory. When these dispersions are transformed into real space in the same way as described in Fig. 2, the energy structure of the electrons in type-II MQWs becomes three subbands (the shaded regions of light blue, medium blue, and deep blue) arise on the quantized energy levels (bottom red lines), as exhibited in Fig. 3(b). As for the band structure of holes in the well of material A, the analysis process is similar. Each quantization energy level of holes is replaced by a band (yellow shaded area) with an energy distribution when all vectors are considered. In addition, the energy bands of holes in material B and electrons in material A without quantum confinement are also displayed in Fig. 3(b) with green and purple shaded areas. It can be concluded that the energies of carriers inside and outside the well both exhibit band-like characteristics with energy distributions when looking through the entire Brillouin zone.

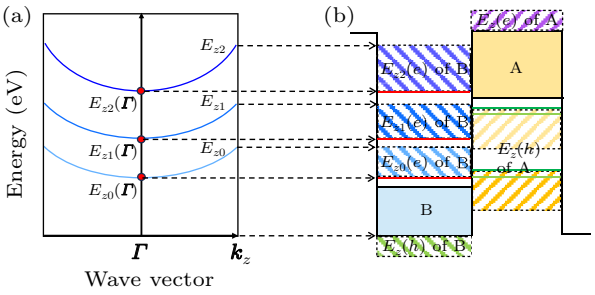


Fig. 3. (a) The schematic diagram of energy dispersions for electrons in the type-II MQWs structure. (b) The energy band structure along the growth direction in the real space for carriers in the type-II MQWs structure from several energy dispersions.

The band structure is the fundamental to studying the properties of low-dimensional materials, and has been successfully used to explain many physical phenomena and help lay the foundation for the designing of micro-/nano-devices. The changes in energy band structure will inevitably lead to a series of chain reactions, including the change of the density of states, the overlap of electron–hole wave function, etc. It is necessary to rebuild the new band theory for the low-dimensional semiconductors to re-understand the physical phenomena and to re-explain the experimental results.

3. Conclusion

In conclusion, a reanalysis of the energy band structure of type-II MQWs has been carried out based on the original

composition of the structure. Unlike the discrete energy levels at a fixed $\boldsymbol{k}$ vector given from the traditional band theory, the energy band structure along the growth direction of carriers in the well exhibits the characteristic of bands with certain energy distribution when all the wave vectors in the entire Brillouin zone are considered. Such a supplementary understanding of the energy band in the two-dimensional quantum well is more comprehensive, which may overturn many viewpoints in traditional band theories and lead to some changes in many parameters, including the density of states, the overlap integration of electron–hole wave function, etc.

Acknowledgments

Project supported by the National Natural Science Foundation of China (Grant Nos. 61991441 and 62004218), the Strategic Priority Research Program of Chinese Academy of Sciences (Grant No. XDB01000000), and Youth Innovation Promotion Association Chinese Academy of Sciences (Grant No. 2021005).

References

[1] Hamaguchi C 2017 *Basic Semiconductor Physics* 3rd Edn. (Switzerland: Springer International Publishing) pp. 1–63
[2] Sharma A and Das T D 2021 *Opt. Mater.* **112** 110734
[3] Benchamekh R, Schulz S and O'Reilly E P 2016 *Phys. Rev. B* **94** 125308
[4] Annathurai S, Chidambaram S, Baskaran B and Venkatesan G K D P 2019 *J. Inorg. Organomet. Polym. Mater.* **29** 535
[5] Das S C, Green R J, Podder J, Regier T Z, Chang G S and Moewes A 2013 *J. Phys. Chem. C* **117** 12745
[6] Margetis J, Al-Kabi S, Du W, Dou W, Zhou Y Y, Pham T, Grant P, Ghetmiri S, Mosle A, Li B H, Liu J F, Sun G, Soref R, Tolle J, Mortazavi M and Yu S Q 2018 *ACS Photonics* **5** 827
[7] Geller C B, Wolf W, Picozzi S, Continenza A, Asahi R, Mannstadt W, Freeman A J and Wimmer E 2001 *App. Phys. Lett.* **79** 368
[8] Rieger M M and Vogl P 1993 *Phys. Rev. B* **48** 14276
[9] Fujimoto Y and Saito S 2016 *Phys. Rev. B* **94** 245427
[10] Grivickas P, McCluskey M D and Gupta 2009 *Phys. Rev. B* **80** 073201
[11] Yan J A, Yang L and Chou M Y 2007 *Phys. Rev. B* **76** 115319
[12] He C, Liu Z, Zhang X, Huang W Q, Xue C L and Cheng B W 2014 *Chin. Phys. B* **23** 116103
[13] Faist J, Capasso F, Sivco D L, Sirtori C, Hutchinson A L and Cho A Y 1994 *Science* **264** 553
[14] Won Y H, Cho O, Kim T, Chung D Y, Kim T, Chung H, Jang H, Lee J, Kim D and Jang E 2019 *Nature* **575** 634
[15] Islam S M, Protasenko V, Lee K, Rouvimov S, Verma J, Xing H L and Jena D 2017 *Appl. Phys. Lett.* **111** 091104
[16] Han C F, Qian R X, Xiang C Y and Qian L 2023 *Chin. Phys. B* **32** 128506
[17] Brum J A and Bastard G 1986 *Phys. Rev. B* **33** 1420
[18] Wu H Y, Ma Z G, Jiang Y, Wang L, Yang H J, Li Y F, Zuo P, Jia H Q, Wang W X, Zhou J M, Liu W M and Chen H 2016 *Chin. Phys. B* **25** 117803
[19] Yang H J, Ma Z G, Jiang Y, Wu H Y, Zuo P, Zhao B, Jia H Q and Chen H 2017 *Sci. Rep.* **7** 43357
[20] Li Y F, Jiang Y, Die J H, Wang C W, Yan S, Wu H Y, Ma Z G, Wang L, Jia H Q Wang W X and Chen H 2018 *Chin. Phys. B* **27** 097104
[21] Sun Q L, Wang L, Jiang Y, Ma Z G, Wang W Q, Sun L, Wang W X, Jia H Q, Zhou J M and Chen H 2016 *Chin. Phys. Lett.* **33** 106801
[22] Liu J, Wang L, Sun L, Wang W Q, Wu H Y, Jiang Y, Ma Z G, Wang W X, Jia H Q and Chen H 2018 *Acta Phys. Sin.* **67** 128101 (in Chinese)
[23] Wang W Q, Wang L, Jiang Y, Ma Z G, Sun L, Liu J, Sun Q L, Zhao B, Wang W X, Liu W M, Jia H Q and Chen H 2016 *Chin. Phys. B* **25** 097307
[24] Li X Z, Sun L, Lu J L, Liu J, Yue C, Xie L L, Wang W X, Chen H, Jia H Q and Wang L 2020 *Chin. Phys. B* **29** 038504
[25] Tang X S, Li X X, Yue C, Wang L, Deng Z, Jia H Q, Wang W X, Ji A C, Jiang Y and Chen H 2020 *Appl. Phys. Express* **13** 071009
[26] Botha J R and Leitch A W R T 1994 *Phys. Rev. B* **50** 18147
[27] Emiliani V, Bonanni B, Frova A, Capizzi M, Martelli F and Stone S S 1995 *J. Appl. Phys.* **77** 5712
[28] Nag B R 2000 *Physics of Quantum Well Devices* (Dordrecht: Kluwer Academic Publishers) pp. 22–34
[29] Milnes A G and Feucht D L 1972 *Heterojunctions and Metal Semiconductor Junctions* (New York: Academic Press) pp. 1–33
[30] Christensen N E 1988 *Phys. Rev. B* **37** 4528
[31] Ketterson J B 2016 *The Physics of Solids* (Oxford City: Oxford University Press) pp. 168–193
[32] Schrödinger E 1926 *Ann. Phys. (Berlin)* **384** 489
[33] Kittel C 1956 *Introduction to Solid State Physics*, 2nd Edn. (New York: John Wiley & Sons) p. 289
[34] Anderson R L 1962 *Solid-State Electron.* **5** 341
[35] Niles D W and Margaritondo G 1986 *Phys. Rev. B* **34** 2923